Disponible en www.hormigonyacero.com
Hormigón y Acero, 2025
https://doi.org/10.33586/hya.2025.3160

ARTÍCULO EN AVANCE ON LINE

An Analytical Model of Simply Supported Steel-Concrete Composite Beam With Bi-Linear Behavior of the Shear Connection Including Ductility: Formulation and Comparison With Numerical Results

Francesco Profico & Zanon Riccardo

DOI: https://doi.org/10.33586/hya.2025.3160

Para ser publicado en: *Hormigón y Acero*

Por favor, el presente artículo debe ser citado así:
Profico, F., Riccardo, Z. (2025) An Analytical Model of Simply Supported Steel-Concrete Composite Beam With Bi-Linear Behavior of the Shear Connection Including Ductility: Formulation and Comparison With Numerical Results, *Hormigón y acero,* https://doi.org/10.33586/hya.2025.3160

Received: Added at production | Revised: Added at production | Accepted: Added at production

DOI: xxx/xxxx

ARTICLE TYPE

An Analytical Model of Simply Supported Steel-Concrete Composite Beam With Bi-Linear Behavior of the Shear Connection Including Ductility: Formulation and Comparison With Numerical Results

Profico Francesco, MSc* | Zanon Riccardo, MSc

[1]Steligence Engineering, ArcelorMittal, Luxembourg

Correspondence
*Francesco Profico, 66, Rue Du Luxembourg, Esch-Sur-Alzette - Luxembourg. Email: francesco.profico@arcelormittal.com

Present Address
66, Rue Du Luxembourg, Esch-Sur-Alzette - Luxembourg

Abstract

An analytical model of simply-supported composite beams is described. A bi-linear law of the shear flow-slip behavior of the shear connection is considered. The influence of the plastic hardening and ductility of the shear connection are included in the model. A formula to predict the end-slip of a generic simply-supported composite beam is derived. The model includes the cases of partial and full shear connection and of elastic and plastic design of the shear connection. The analytical model predictions are compared and checked against the results of a one-dimensional numerical model of composite beam including non-linearity. The comparison reveals a substantial agreement between the novel analytical formulas and the numerical model.

KEYWORDS:
Composite beams; Shear connection; Analytical model; End-slip; Partial-shear

1 | INTRODUCTION

Composite steel-concrete beams are in the European framework designed according to Eurocode 4[1] (EC4). These can be used both for buildings and bridges. The design of the shear connection can be in general elastic or plastic[2]. While in the case of composite bridges design only a slight plastic redistribution is admitted, in the case of buildings EC4 opens to a plastic design of the shear connection. The design of elements in partial shear connection is highly affected by the resistance of the shear connection itself[3]. The reduction of bending resistance of the section must be considered with the use of the Partial Shear Diagram. The slip demand on the shear connection is higher as the shear connection yields approaching the member ultimate load. In the case of plastic design ductile shear connectors must be used. EC4 defines ductile shear connectors as the ones reaching a minimum plastic slip of 6 mm. Typically headed stud shear connectors are used as shear connectors as the ductility requirement imposed by EC4 is satisfied and specific design rules are provided already by the codes. The design of composite beams can be done both in full and partial shear connection. The degree of shear connection η is a key parameter to predict the composite beam behaviour. EC4 imposes limitations to the use of partial shear connection in buildings. A minimum degree of shear connection is imposed by EC4. These limitations are strictly calibrated for the value of 6 mm of slip capacity. The minimum degree of shear connection mainly depends on section symmetry, the steel yield resistance and the composite beam member length. These limitations are more severe for longer elements. The limitations are more strict for more asymmetric beams and higher steel grades. The limit exists mainly because in a low degree of shear connection a higher plastic deformation capacity is required to the shear connection. If a simply supported beam is considered, the highest plastic slip capacity is required

at the end of the beam. The beam end-slip is generally observed to sharply increase as the ultimate bearing capacity of the beam is approached. The slip demand becomes more severe for lower degree of shear connection. In order to guarantee a consistent structural design of the composite beam, EC4 introduces limitations in terms of minimum degree of shear connection. This to prevent that, for low degree of shear connection the slip demand on the shear connection is higher compared with the plastic slip capacity minimum threshold of 6 mm. Some observations in numerical analysis were done in[4] with the purpose to propose a slip-capacity dependent formulation, taking into account the effect of highly asymmetric steel part sections.

The plastic calculation is done assuming a rigid-plastic behavior of the shear connection. This leads to the introduction of the concept of degree of shear connection. The consistency of this assumption heavily relies on the fact that typical shear connection means as head-studs show a high ductility with low hardening ratio. Hence, the hypothetical rigid-plastic behavior is effectively well representing this behavior. From a rigid-plastic behavior is however not possible to derive an estimation of the slip demand. Analytically derived formulations to predict this are at the current state missing. The influence of parameters like the first yield slip, the ductility of the shear connection and the hardening ratio in the plastic branch are at the current state missing. A model providing analytical formulations and correctly linking the limit cases of perfectly elastic connection and rigid-plastic connection is at the current state not existing. This would be of extreme interest especially in the frame of the elaboration of the forthcoming next generation version of EC4. This in fact will generalize the design, facilitating the calculation process for different connection means compared to head-studs and trying to correctly include the effect of mechanical behaviors highly different from rigid-plastic ones.

Analytical methods describing the mechanical behaviour of a composite beam exist already[5]. In the present article a specific one is presented which main aim is to describe the influence of key parameters as the shear connection ductility, ultimate slip and the plastic hardening. This is done considering the effect of the load ratio and the degree of shear connection. The results predicted by the derived formulations are compared with the respective ones obtained from a one-dimensional finite-difference method of a composite beam implementing both the shear connection non-linearity and the cross-section non-linearity. For this implementation reference to[6] is made.

2 | REVIEW OF COMPOSITE BEAMS MECHANICS

Composite steel-concrete beams are structural elements composted by a concrete and a steel part. These are connected by means of a shear connection. The shear connection transfers longitudinal shear. It allows for reaching the composite action of the two parts.

The mechanical behavior of the shear connection strongly affects the mechanical behavior of the composite element. Concrete and steel materials can exhibit non-linear behavior. The shear connection can show non-linear behavior as well.

2.1 | Kinematic compatibility and equilibrium equations of shear connection

For *equilibrium* on the concrete part, a variation in the *concrete compression force* N_c is balanced by the presence of a *longitudinal shear* v_L. In Equation 1 the equilibrium is expressed in differential and integral form.

$$\frac{dN_c(x)}{dx} = -v_L(x) \quad \leftrightarrow \quad N_c(x) = N_c(x_0) - \int_{x_0}^{x} v_L(x')\,dx' \tag{1}$$

Note that a distinction between x and x' is used only for mathematical formality, distinguishing the function variable from the integration variable respectively.

For kinematic *compatibility* the derivative of *slip* δ is related with the *slip strain* ϵ_{slip}. The relation is described by Equation 2 in differential and integral form.

$$\frac{d\delta(x)}{dx} = \epsilon_{slip}(x) \quad \leftrightarrow \quad \delta(x) = \delta(x_0) + \int_{x_0}^{x} \epsilon_{slip}(x')\,dx' \tag{2}$$

2.2 | Connection shear flow-slip behaviour

The shear connection is generally composed by shear connectors. These can be arranged in more than one line and present non-uniform spacing. In the present article a constant number of lines is assumed along the beam. Moreover, a uniform spacing e_x of connectors is assumed.

The number of rows of shear connectors present between the mid-span and the support section is calculated according to Equation 3:

$$n = \frac{L/2}{e_x} \tag{3}$$

Shear connectors have in general a non-linear shear force-slip behavior $P - \delta$ (Equation 4).

$$P(\delta) \qquad \text{Shear force-slip behavior of connector} \tag{4}$$

A shear flow-slip behaviour of the shear connection is defined by dividing the shear force-slip law of the uniformly spaced lines of connectors by the spacing e_x, properly considering the number of connectors present in a line (Equation 5).

$$v_L(\delta) = \frac{P(\delta)}{e_x} \qquad \text{Shear flow-slip behavior of shear connection} \tag{5}$$

If the yield force of the shear connector is denoted as P_y, a yield shear flow can be defined as Equation 6.

$$v_{L,y} = \frac{P_y}{e_x} \qquad \text{Yield shear flow} \tag{6}$$

2.3 | Composite section behaviour

The characterisation of the composite section mechanical behaviour can be done via a Strain Limited (SL) analysis. The research[6] is used as reference. A linear distribution of strains is assumed on the two parts of the section. The deformation state is described by the strain slip ϵ_{slip}, the curvature $(1/r)$ and by specifying an additional strain ϵ_0 for one fibre of the section. The stress distributions are consequence of $\sigma - \epsilon$ laws associated to the materials. The resultants of the bending moment M and axial force N are derived by integrating the stress distributions over the section under a defined deformation state. The number of free parameters reduces to two by imposing the condition of pure bending $N = 0$. The composite section behaviour is described by a surface (Equation 7). This surface is named *Partial Shear Surface* (PSS). Both the concrete compression N_c and the moment resultant on the section can be expressed as function of the kinematic variables slip strain ϵ_{slip} and curvature $(1/r)$.

$$\begin{cases} M(\epsilon_{slip}, (1/r)) = M(\epsilon_{slip}(x), (1/r)(x)) \\ N_c(\epsilon_{slip}, (1/r)) = N_c(\epsilon_{slip}(x), (1/r)(x)) \end{cases} \tag{7}$$

If the surface has monotonic behavior, the relation can be inverted. The slip strain ϵ_{slip} and the curvature $(1/r)$ can be described by Equation 8).

$$\begin{cases} \epsilon_{slip}(M, N_c) = \epsilon_{slip}(M(x), N_c(x)) \\ (1/r)(M, N_c) = (1/r)(M(x), N_c(x)) \end{cases} \tag{8}$$

In conditions of Full Shear Interaction (FSI) the slip strain ϵ_{slip} is zero. The Ultimate Limit State of the section is dependent on the slip strain ϵ_{slip}. The associated ultimate curvature is $(1/r)_u(\epsilon_{slip})$. At Ultimate Limit State (ULS) in FSI conditions the quantities of Equation 9 can be defined.

$$M_{pl,f} = M(\epsilon_{slip} = 0, (1/r)_u) \tag{9}$$

$$N_{cf} = N_{cf}(\epsilon_{slip} = 0, (1/r)_u) \tag{10}$$

The *Partial Shear Diagram* (PSD) is composed by the set of points $M(\epsilon_{slip}), N_c(\epsilon_{slip})$ in the $M - N_c$ plane. These points are ULS points derived with ultimate curvature $(1/r)_u$. This is a function of the strain slip ϵ_{slip}. These points are derived as function of the parameter ϵ_{slip} Equation 11:

$$\begin{cases} M(\epsilon_{slip}) = M((\epsilon_{slip}, (1/r)_u(\epsilon_{slip}))) \\ N_c(\epsilon_{slip}) = N_c((\epsilon_{slip}, (1/r)_u(\epsilon_{slip}))) \end{cases} \tag{11}$$

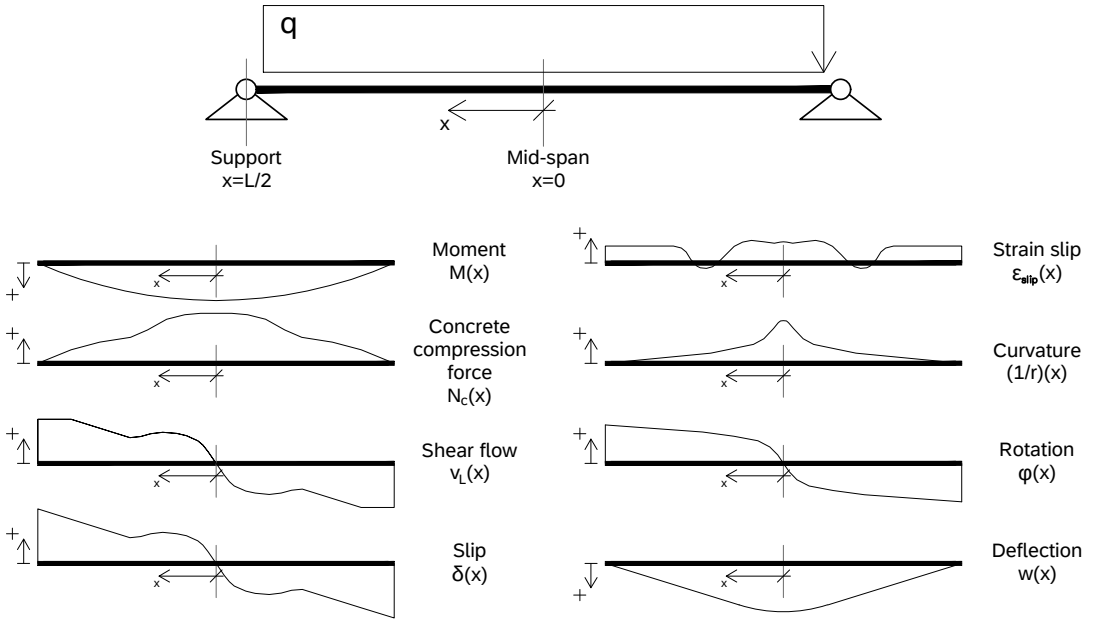

Figure 1 static scheme of the simply supported composite beam with reference system. Below a qualitative example of the relevant distributions is shown.

2.4 | Degree of shear connection

The composite section experiences a force on the concrete part $N_c(x = L/2)$ at mid-span. In the support region no external force is applied on the concrete part. The boundary condition $N_c(x = L/2) = 0$ should be satisfied. For equilibrium reasons the shear connection transfers a force of N_c between the mid-span section and the support section. The mean shear flow is $N_c/(L/2)$. The degree of shear connection is defined as Equation 12:

$$\eta = \frac{n}{n_f} = \frac{n \cdot P_y}{N_{cf}} \tag{12}$$

In Full Shear Connection cases (FSC) the connection is sufficiently resistant to transfer the force N_{cf}. Namely (Equations 13 and 14):

$$\eta = \frac{n \cdot P_y}{N_{cf}} \geq 1 \qquad \text{FULLS SHEAR CONNECTION (FSC)} \tag{13}$$

In the opposite case the shear connection is not sufficiently resistant to transfer the force:

$$\eta = \frac{n \cdot P_y}{N_{cf}} < 1 \qquad \text{PARTIAL SHEAR CONNECTION (PSC)} \tag{14}$$

By substituting Equation 6 and Equation 3 in Equation 12, the relation of Equation 15 is derived:

$$N_{cf} = \frac{1}{\eta} \cdot \frac{L \cdot v_{L,y}}{2} \tag{15}$$

3 | ANALYTICAL MODEL FORMULATION

3.1 | Assumptions

The model is based on the following assumptions:

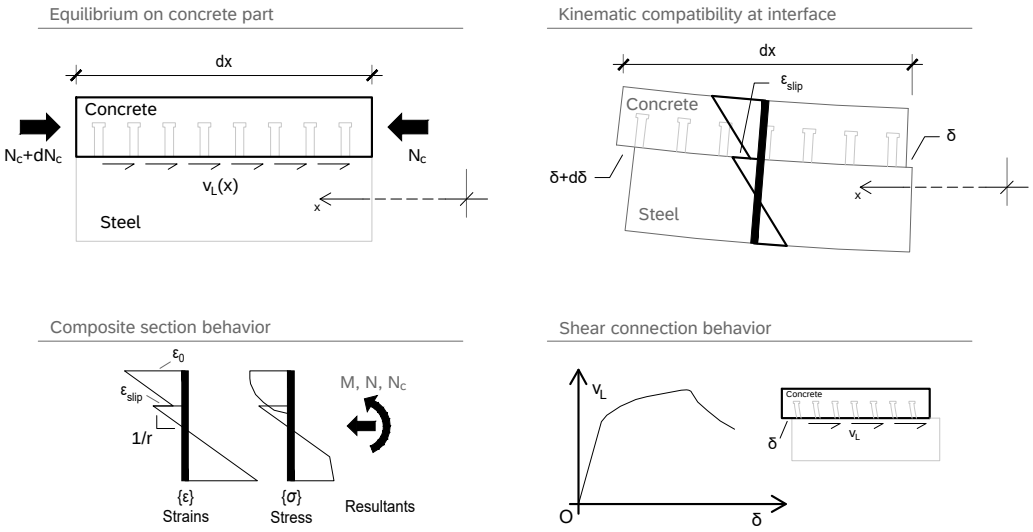

Figure 2 basic principles governing the mechanical behavior of the composite beam

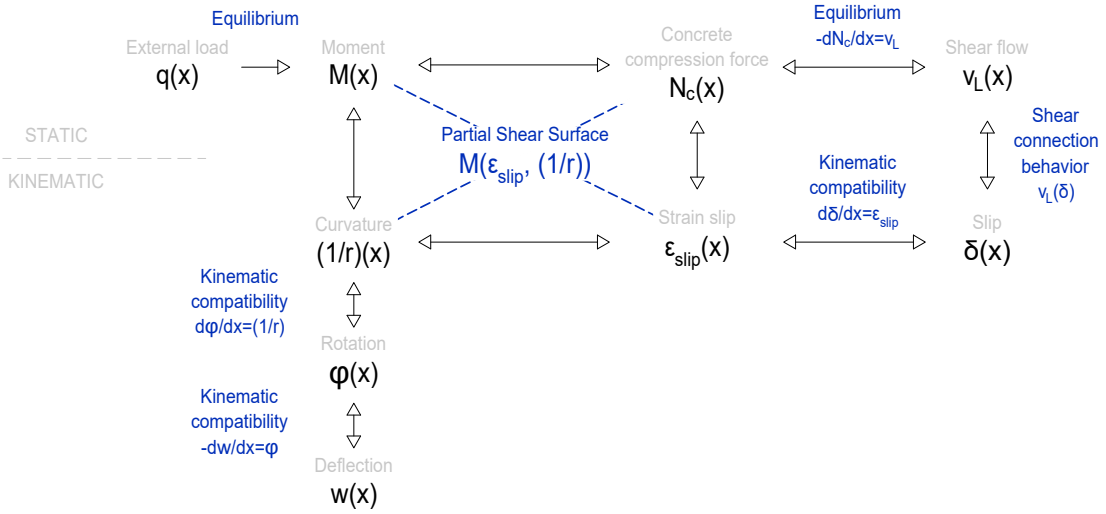

Figure 3 schematic representation of the theory governing the mechanical behavior of the simply supported composite element. The coupling of the different distribution is described

- A simply supported element of span-length L is considered with degree of shear connection η. The composite section of the element is constant. In Full Shear Interaction at ULS the resultant compression force on the concrete part is N_{cf}.
- A constant slip strain along the beam is assumed. Namely (Equation 16):

$$\epsilon_{slip}(x) = \overline{\epsilon}_{slip} = \text{const.} \tag{16}$$

  This constitutes a strong simplification hypothesis.
- The shear connection behaviour is described by a bi-linear model. In correspondence of the slip δ_y the yield point is reached and the shear flow is $v_{L,y}$. The hardening factor β is the ratio between the post-yield stiffness and the first elastic

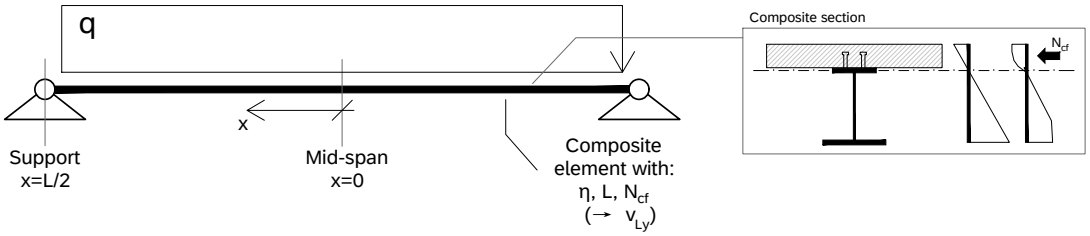

Figure 4 relevant parameters used as reference, static scheme and reference system used in the elaboration of the analytical model

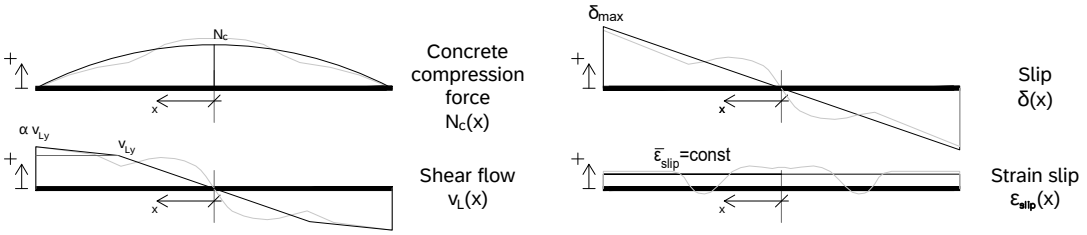

Figure 5 simplification hypothesis of constant strain slip ϵ_{slip} and influence on the other distributions. A bi-linear mechanical model of the shear connection is used.

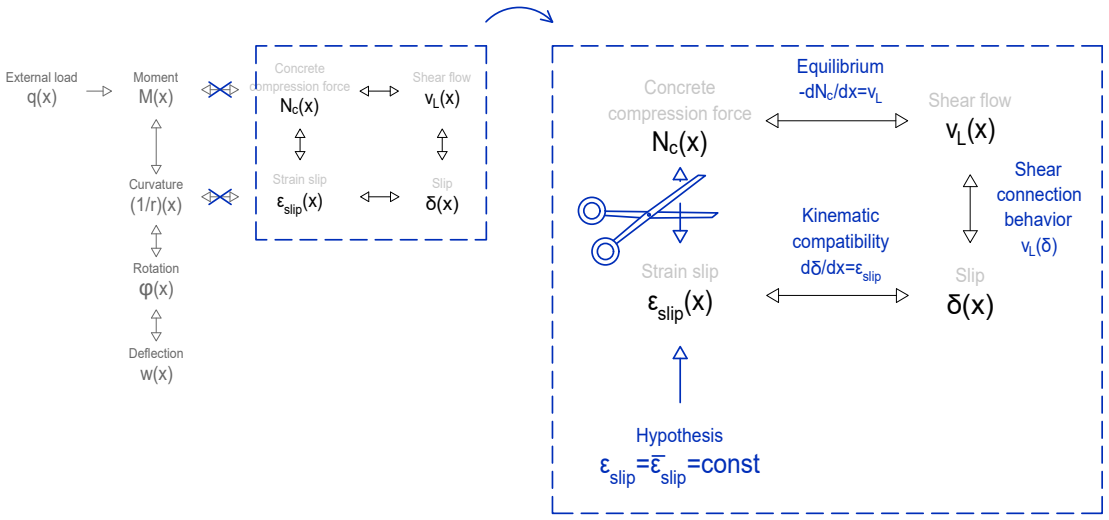

Figure 6 observed ductility values for the given shape

branch stiffness. The law is described by Equation 17:

$$v_L(\delta) = \begin{cases} \frac{v_{L,y}}{\delta_y} \cdot \delta & \delta < \delta_y \\ v_{L,y} + \beta \cdot \frac{v_{L,y}}{\delta_y} \cdot (\delta - \delta_y) & \delta \geq \delta_y \end{cases} \tag{17}$$

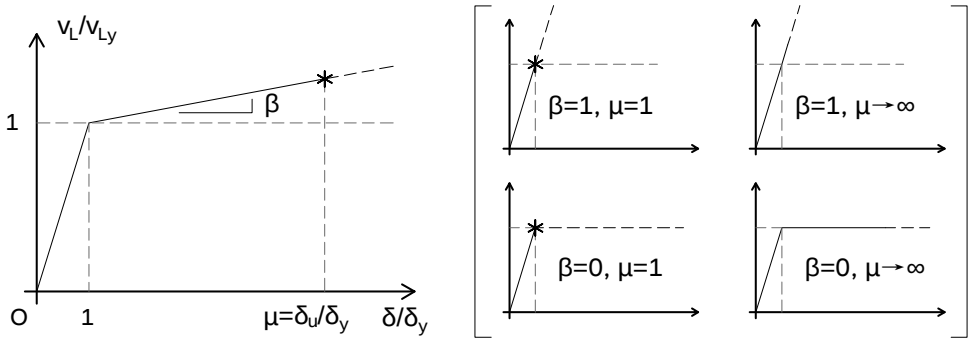

Figure 7 Bi-linear mechanical shear flow-slip model of the shear connection and related limit cases

- the parameter δ_u defines a limit of slip for the shear connection. At this slip the shear connection reaches failure. The ductility is defined as the ratio $\mu = \delta_u/\delta_y$.

- at mid-span a concrete compression force N_c is applied on the section. For equilibrium (Equation 1), applying the proper boundary conditions, the following condition should be satisfied (Equation 18). A loading ratio r describes the loading level. This is defined as the ratio between the applied force N_c and the one corresponding to ULS in FSI conditions, namely:

$$\int_{x=0}^{x=L/2} v_L(x)\, dx = N_c = r \cdot N_{cf} \tag{18}$$

As consequence of the these hypothesis the slip varies linearly between the mid-span section and the support section (Equation 19):

$$\delta(x) = \overline{\epsilon}_{slip} \cdot x \tag{19}$$

In case $\delta_{max} \geq \delta_y$ the shear connection is yielded. In this case the coordinate where the coordinate x_y where yield is reached, closer to mid-span can be computed by equating $\delta_y = \delta(x)$, thus deriving x_y from Equation 20.

$$x_y = \delta_y/\overline{\epsilon}_{slip} \tag{20}$$

The parameter ζ is introduced as Equation 21. This parameter represents the *non-dimensional elastic length*.

$$\zeta = \frac{\delta_y/\epsilon_{slip}}{L/2} \tag{21}$$

In cases $\zeta > 1$ the shear connection is in the elastic phase. In case $\zeta \leq 1$, the shear connection is yielded. The end-slip δ_{max} can be computed as Equation 23):

$$\delta_{max} = \overline{\epsilon}_{slip} \cdot L/2 \tag{22}$$

From the mean-value theorem of calculus:

$$\delta_{max} = \delta(x=0) + \int_{x'=0}^{x'=L/2} \epsilon_{slip}(x')\, dx' = \delta(x=0) + \overline{\epsilon}_{slip} \int_{x'=0}^{x'=L/2} dx' = \overline{\epsilon}_{slip} \cdot L/2 \tag{23}$$

Note: a distinction between x and x' is used only for mathematical formality, distinguishing the function variable from the integration variable respectively. Therefore, the calculation of the end-slip δ_{max} under hypotheses 16 and the integral coming from a generic distribution ϵ_{slip} from calculus, coincide. If the model is able to exactly estimate the mean strain slip $\overline{\epsilon}_{strain}$, the

model would deliver a correct estimation of the end-slip δ_{max}. As consequence of the two assumptions 16 and 5, the shear flow varies along the coordinate as described by Equation 24:

$$v_L(x) = v_L(\delta(x)) = \begin{cases} \frac{v_{L,y}}{\delta_y} \cdot \overline{\epsilon}_{slip} \cdot x & x < \delta_y/\overline{\epsilon}_{slip} \\ v_{L,y} + \beta \cdot \frac{v_{L,y}}{\delta_y} \cdot (\overline{\epsilon}_{slip} \cdot x - \delta_y) & x \geq \delta_y/\overline{\epsilon}_{slip} \end{cases} \tag{24}$$

The *shear-flow over-strength at support* is denoted as α and is hereby defined as Equation 25:

$$\alpha = \frac{v_L(x = L/2)}{v_{L,y}} = \frac{v_L(\delta(x = L/2))}{v_{L,y}} \tag{25}$$

The *non-dimensional integral of the shear flow-slip model* is defined (Equation 26).

$$\Psi(\mu, \beta) = \frac{1}{v_{L,y} \cdot \delta_u} \int_{\delta=0}^{\delta=\delta_u} v_L(\delta)\, d\delta = \frac{\beta(\mu^2 - 2\mu + 1) + 2\mu - 1}{2\mu} \tag{26}$$

The non-dimensional integral of the shear flow-slip model assumes the values (Equation 27):

$$\begin{cases} \Psi(\mu = 1, \beta) = 1/2 \\ \Psi(\mu \to \infty, \beta = 0) \to 1 \\ \Psi(\mu \to \infty, \beta > 0) \to \infty \end{cases} \tag{27}$$

The *non-dimensional capacity of shear connection respect to the applied force* is defined (Equation 28). This can be linked to the non-dimensional integral of the shear flow-slip model and the degree of shear connection using Equations 15 and 26.

$$\eta^*(\beta, \eta, \mu) = \frac{1}{N_{cf}} \cdot \int_{x=0}^{x=L/2} v_L(x) dx = \eta \cdot \Psi(\mu, \beta) \tag{28}$$

The non-dimensional capacity of shear connection assumes the values (Equation 29):

$$\begin{cases} \eta^*(\beta > 0, \mu \to \infty) \to \infty \\ \eta^*(\beta = 0) = \left(\frac{2\mu - 1}{2\mu}\right) \cdot \eta \\ \eta^*(\beta = 0, \mu \to \infty) = \eta \\ \eta^*(\beta \geq 0, \mu = 1) = \frac{1}{2} \cdot \eta \\ \eta^*(\beta = 0, \mu = 2) = \frac{3}{4} \cdot \eta \end{cases} \tag{29}$$

In the case $\beta = 0$ with $\mu \to \infty$, the notion of non-dimensional capacity of shear connection is coincident with the degree of shear connection. This reflects the case of rigid-plastic behavior of the shear connection with infinite ductility.

The *maximum concrete compression force transferable by the shear connection* $N_{c,max}$ is (Equation 30):

$$N_{c,max}(\beta, \eta, \mu) = \begin{cases} N_{cf} & \eta^* \geq 1 \\ \eta^*(\beta, \eta, \mu) N_{cf} & \eta^* < 1 \end{cases} \tag{30}$$

The *resistant bending moment of the composite element* M_R is (Equation 31):

$$M_R(\beta, \eta, \mu) = f(N_{c,max}(\beta, \eta, \mu)/N_{cf}) \cdot M_{pl,f,R} \tag{31}$$

Here the function $f(N_c/N_{cf}) \cdot M_{pl,f,R}$ represents the PSD.

3.2 | Model formulation without slip limitation

The condition of no slip limitation is assumed. It is considered that the ultimate slip δ_u tends to infinite as well as the ductility μ. Namely (Equation 32):

$$\mu \to \infty \qquad \delta_u = \mu \cdot \delta_y \to \infty \tag{32}$$

3.2.1 | Case $\eta/r \geq 2$

The applied force on the concrete part at mid-span is $N_c = r \cdot N_{cf}$. Here, N_{cf} can be expressed using Equation 15. The maximum applied force is $N_c \leq v_{L,y} \cdot L/4 \leq N_{cf}$. The shear connection is in the elastic phase $\delta < \delta_y$ (or equivalently $\zeta > 1$). The equilibrium condition is described by Equation 33 starting from Equations 18, 19 and 24:

$$\frac{1}{2}\frac{v_{L,y}}{\delta_y} \cdot \overline{\epsilon}_{slip} \cdot (L/2)^2 = \frac{r}{\eta} \cdot v_{L,y} \cdot \frac{L}{2} \tag{33}$$

The equation can be written in non-dimensional terms (Equation 34). This is done by dividing the left-hand side and the right-hand side by $v_{L,y} \cdot L/2$. The particular value of ζ satisfying the equilibrium condition (Equation 33) can be derived inverting the relation.

$$\frac{1}{2\zeta} = \frac{r}{\eta} \qquad \rightarrow \qquad \zeta = \frac{\eta}{2r} \tag{34}$$

From Equations 21, 23 and 25 follows:

$$\overline{\epsilon}_{slip} = 4r \cdot \frac{\delta_y}{\eta L} \qquad \rightarrow \qquad \delta_{max} = \overline{\epsilon}_{slip} \cdot L/2 \qquad \rightarrow \qquad \alpha = \frac{v_L(\delta_{max})}{v_{L,y}} = \frac{2 \cdot r}{\eta} \tag{35}$$

Since the shear connection is not in the plastic phase, the solution is not dependent from the parameter of hardening β.

3.2.2 | Case $1 \leq \eta/r < 2$

The applied force on the concrete part at mid-span is $N_c = r \cdot N_{cf}$. Here, N_{cf} can again be expressed using Equation 15. The maximum applied force is $v_{L,y} \cdot L/4 < N_c \leq v_{L,y} \cdot L/2$. The shear connection yields $\delta > \delta_y$ (or equivalently $\zeta < 1$). The equilibrium condition is described by Equation36 starting from Equations 18, 19 and 24:

$$\frac{1}{2}\frac{\delta_y}{\overline{\epsilon}_{slip}} \cdot v_{L,y} + v_{L,y} \cdot \left(\frac{L}{2} - \frac{\delta_y}{\overline{\epsilon}_{slip}}\right) + \beta \cdot v_{L,y}\left(\frac{\delta_y}{\overline{\epsilon}_{slip}} - \frac{L}{2}\right) + \beta \cdot \frac{v_{L,y}}{2\delta_y} \cdot \overline{\epsilon}_{slip} \cdot \left(\left(\frac{L}{2}\right)^2 - \left(\frac{\delta_y}{\overline{\epsilon}_{slip}}\right)^2\right) = \frac{r}{\eta} \cdot v_{L,y} \cdot \frac{L}{2} \tag{36}$$

The equation can be written in non-dimensional terms (Equation 37). This is done by dividing the left-hand side and the right-hand side by $v_{L,y} \cdot L/2$.

$$\frac{1}{2\zeta} + (1-\zeta) + \beta(\zeta - 1) + \frac{\beta}{2\zeta}(1-\zeta^2) = \frac{r}{\eta} \tag{37}$$

The equation expresses the equilibrium condition. The parameter ζ has to satisfy Equation 37. It is assumed $\zeta \neq 0$. It can be rewritten in the canonical form $a\zeta^2 + b\zeta + c = 0$. This represents a second order equation in the parameter ζ (Equation 37), which roots are:

$$\zeta_{1,2} = \frac{-b \pm \sqrt{b^2 - 4ac}}{2a} \qquad a = \frac{1}{2}(\beta - 1) \qquad b = 1 - \beta - r/\eta \qquad c = \beta/2 \tag{38}$$

The solution of interest is described by Equation 39.

$$\zeta(\beta, \eta, r) = \frac{1 + \beta\eta/r - \eta/r - \sqrt{-\beta\eta^2/r^2 + 2\beta\eta/r + \eta^2/r^2 - 2\eta/r + 1}}{\eta/r(\beta - 1)} \tag{39}$$

From Equations 21, 23 and 25 follows:

$$\overline{\epsilon}_{slip}(\beta, \eta, r) = \frac{2}{\zeta(\beta, \eta, r)} \cdot \frac{\delta_y}{L} \qquad \rightarrow \quad \delta_{max}(\beta, \eta, r) = \overline{\epsilon}_{slip}(\beta, \eta, r) \cdot L/2 \qquad \rightarrow \quad \alpha(\beta, \eta, r) = \frac{v_L(\delta_{max}(\beta, \eta, r))}{v_{L,y}} \tag{40}$$

3.2.3 | Case $\eta/r < 1$

The parameter β is assumed strictly positive $\beta > 0$. It is possible to find an equilibrium configuration (i.e. a solution of ζ) that still satisfies Equation 36. The applied force on the concrete part at mid-span is $N_c = r \cdot N_{cf}$ and can be expressed using Equation 15. The same conclusions of the case $1 \leq \eta < 2$ are made. The only difference is in the fact that β is strictly positive. The considered case is ideal. A bi-linear model of the shear connection is assumed with a positive hardening $\beta > 0$. No slip limitation is assumed. Assuming this ideal law with indefinite limit of the plastic branch, a solution exists to the equilibrium equation assuming $N_c \leq N_{cf}$ as boundary condition.

3.2.4 | Limit cases

Case $\beta = 0$

If $\beta = 0$ is assumed, Equation 39 becomes Equation 41.

$$\zeta = \frac{1 - \eta/r - \sqrt{\eta^2/r^2 - 2\eta/r + 1}}{-\eta/r} = \frac{|1 - \eta/r| - (1 - \eta/r)}{\eta/r} = \begin{cases} \frac{2(\eta/r-1)}{\eta/r} & \eta/r > 1 \\ 0 & \eta/r \leq 1 \end{cases} \tag{41}$$

The second case of Equation 41 is in contrast with the assumption of $\zeta \neq 0$. The solution is not accepted. This result reflects the fact that for $\beta = 0$, is not possible to find an equilibrium configuration in case $\eta/r \leq 1$. The limit of the value of the integral of the shear flow on the beam tends to $v_{L,y} \cdot L/2$.

Limit $\beta \to 0$

In the limit $\beta \to 0$, the root ζ tends to the values presented in Equation 41. Consequently, the parameters α and δ_{max} can be demonstrated to tend to those of Equation 42.

$$\alpha(\beta \to 0, \eta/r) = \lim_{\beta \to 0} \left(1 + \beta(\frac{1}{\zeta(\beta, \eta/r)} - 1)\right) = \begin{cases} 1 & \eta/r > 1 \\ \frac{2-\eta/r}{\eta/r} & \eta/r \leq 1 \end{cases} \tag{42}$$

$$\left(\frac{\delta_{max}}{\delta_y}\right)(\beta \to 0, \eta/r) = \lim_{\beta \to 0} \left(\frac{1}{\zeta}\right) = \begin{cases} \frac{\eta/r}{2\eta/r-2} & \eta/r > 1 \\ \text{solution does not exist} & \eta/r \leq 1 \end{cases} \tag{43}$$

Limit $\beta \to 1$

In the limit $\beta \to 1$, the root ζ tends to the value $\eta/r/2$. This can be demonstrated analytically using the De L'Hopital theorem of calculus. Consequently, the parameters α and δ_{max} can be demonstrated to tend to those of Equation 44.

$$\alpha(\beta \to 1, \eta/r) = \lim_{\beta \to 1} \left(1 + \beta(\frac{1}{\zeta(\beta, \eta/r)} - 1)\right) = \frac{2r}{\eta} \tag{44}$$

$$\left(\frac{\delta_{max}}{\delta_y}\right)(\beta \to 1, \eta/r) = \lim_{\beta \to 1} \left(\frac{1}{\zeta}\right) = \frac{2r}{\eta} \tag{45}$$

3.3 | Model formulation including slip limitation

The slip limitation is reintroduced (Equation 46). The ductility μ is considered to be finite.

$$\mu << \infty \qquad \delta_u = \mu \cdot \delta_y << \infty \tag{46}$$

The end-slip δ_{max} is limited to the value δ_u. The condition defines a limitation to the value of ζ. By introducing Equations 21 and 46:

$$\frac{\delta_{max}}{\delta_y} = \frac{\overline{\epsilon}_{slip} L/2}{\delta_y} = 1/\zeta \leq \mu = \frac{\delta_u}{\delta_y} \tag{47}$$

This imposes a lower bound to the value of ζ. From this condition, Equation 53 holds:

$$\zeta \geq \zeta'' = 1/\mu \tag{48}$$

The criteria to define ζ that includes the slip limitation (Equation 46) is the one of Equation 49:

$$\zeta(\beta, \eta/r, \mu) = \max\left(\zeta'(\beta, \eta, r), \zeta''(\mu)\right) \tag{49}$$

Here the parameter ζ' is the one from Equation 39 and the parameter ζ'' comes from Equation 53. The two different cases can be identified:

$$\begin{cases} \zeta = \zeta' & \text{or} \quad \zeta' > \zeta'' & \text{Failure of the composite section} \\ \zeta = \zeta'' & \text{or} \quad \zeta' < \zeta'' & \text{Failure of the shear connection} \end{cases} \tag{50}$$

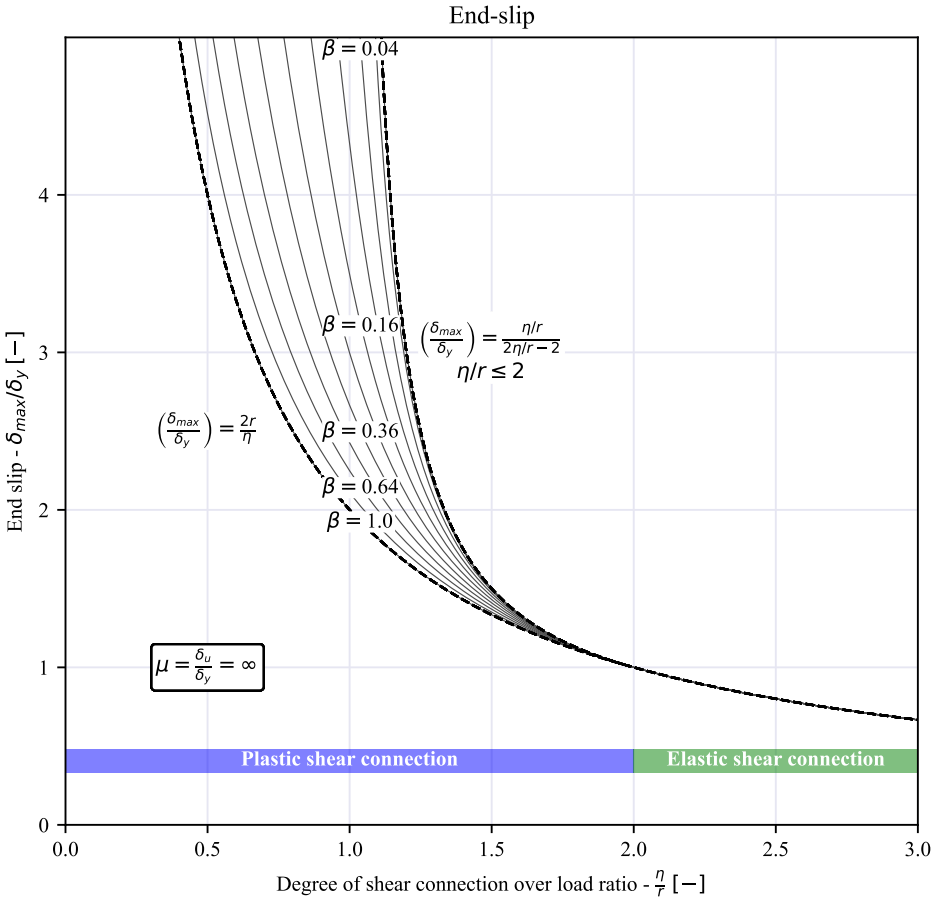

Figure 8 Resulting graph for the end-slip as function of the ratio η/r for different values of the parameter β.

The end-slip and the over strength of the shear flow at support are calculated from Equations 23, 21 and 53.

$$\left(\frac{\delta_{max}}{\delta_y}\right)(\beta, \eta, r, \mu) = \begin{cases} \frac{1}{\zeta(\beta,\eta,r,\mu)} & 0 \leq \eta/r < 2 \\ 2r/\eta & \eta/r \geq 2 \end{cases} \tag{51}$$

$$\alpha(\beta, \eta, r, \mu) = \begin{cases} 1 + \beta\left(\frac{1}{\zeta(\beta,\eta,r,\mu)} - 1\right) & 0 \leq \eta/r < 2 \\ 2r/\eta & \eta/r \geq 2 \end{cases} \tag{52}$$

The non-dimensional capacity of shear connection η^* is calculated according to Equation 28.

In figure 10 the different graphs as function of the parameters β, η, r, are illustrated for a particular value of ductility μ.

3.3.1 | Limit cases

Case $\mu = 1$

In case of $\mu = 1$ ($\delta_u = \delta_y$), the shear connection has no redistribution capacity. In figure 11 the different graphs for this case are described. The overstrength factor α can assume a maximum value of $\alpha = 1$. The maximum transmissible force $N_{c,max}$ of the shear connection is $N_{c,max} = v_{L,y}L/4$. The end-slip δ_{max} is limited to δ_y. The load capacity of the composite element is limited by the limited capacity of the shear connection already for $\eta \leq 2$.

Case $\mu \to \infty$

In case of $\mu \to \infty$, the shear connection has large redistribution capacity. In figure 12 the different graphs for this case are described. In the case $\beta = 0$ the maximum overstrength factor α assumes value $\alpha = 1$. This case coincides with a rigid-plastic shear connection with infinite redistribution capacity. In this case the notion of the parameter η^* coincides with the notion of

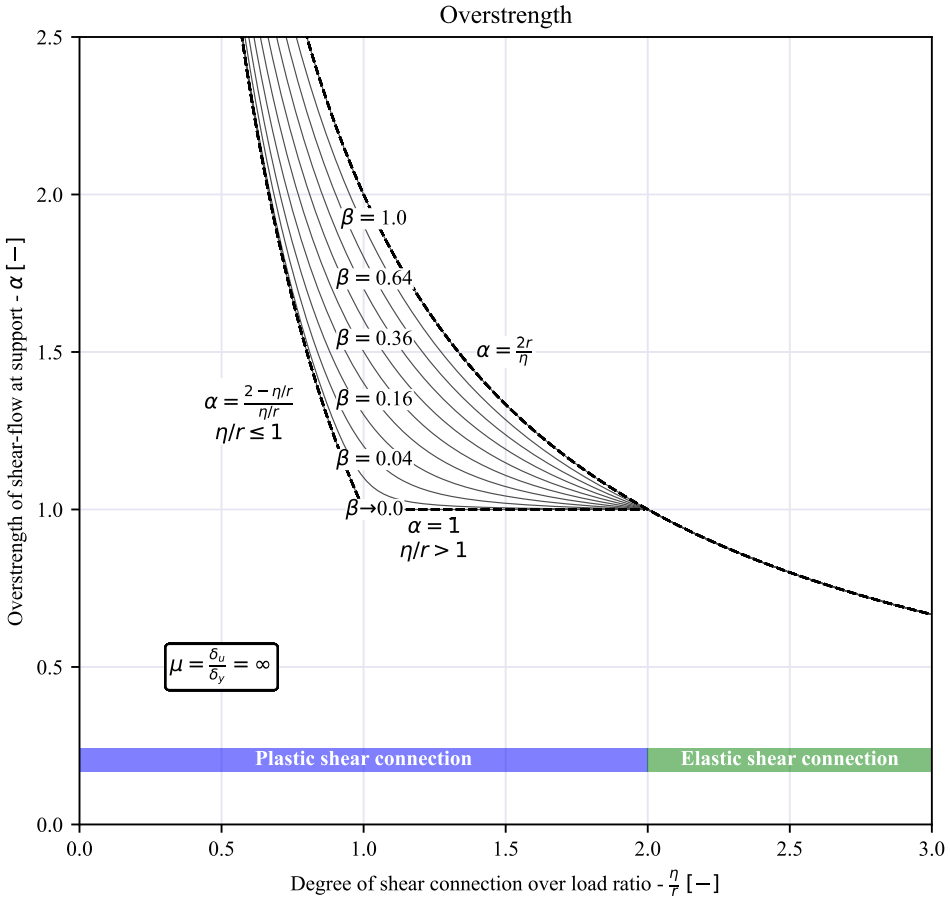

Figure 9 Resulting graph for the over-strength α as function of the ratio η/r for different values of the parameter β.

degree of shear connection. The ratio between the two is unitary. The rigid plastic case with no limitation has two different interpretations. The first is δ_u being reasonable and δ_y being much smaller $\delta_y << \delta_u$. The second interpretation is δ_y having reasonable values with δ_u significantly larger $\delta_u >> \delta_y$. The two cases are in the present model equivalent. The decisive parameter is in fact the ductility μ. For $\beta \to 0$ but with strictly positive values $\beta > 0$, the value of Ψ of the shear connection tends to infinite. This means that an equilibrium solution can be found that balances the force N_{cf}. This is valid as well for values $\eta/r < 1$.

3.4 | Model summary

In figure 13 the analytical scheme is summarized. The analytical formulation of the various parameters are presented below.

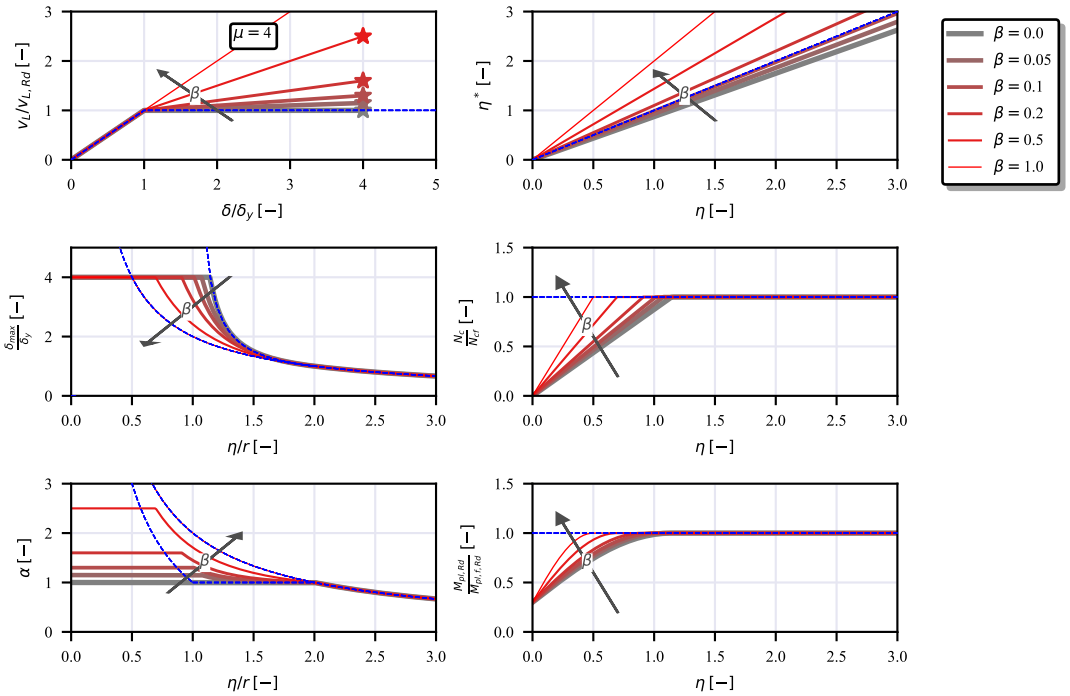

Figure 10 Resulting graphs for variable values of β for a specified value of ductility $\mu = 4$. Note that as function f of the PSD a specific function is proposed, thus consisting in an example. Therefore the $M_{pl,Rd}$ vs η graph can not be applied generally but specifically relates to the composite section studied and the related PSD function.

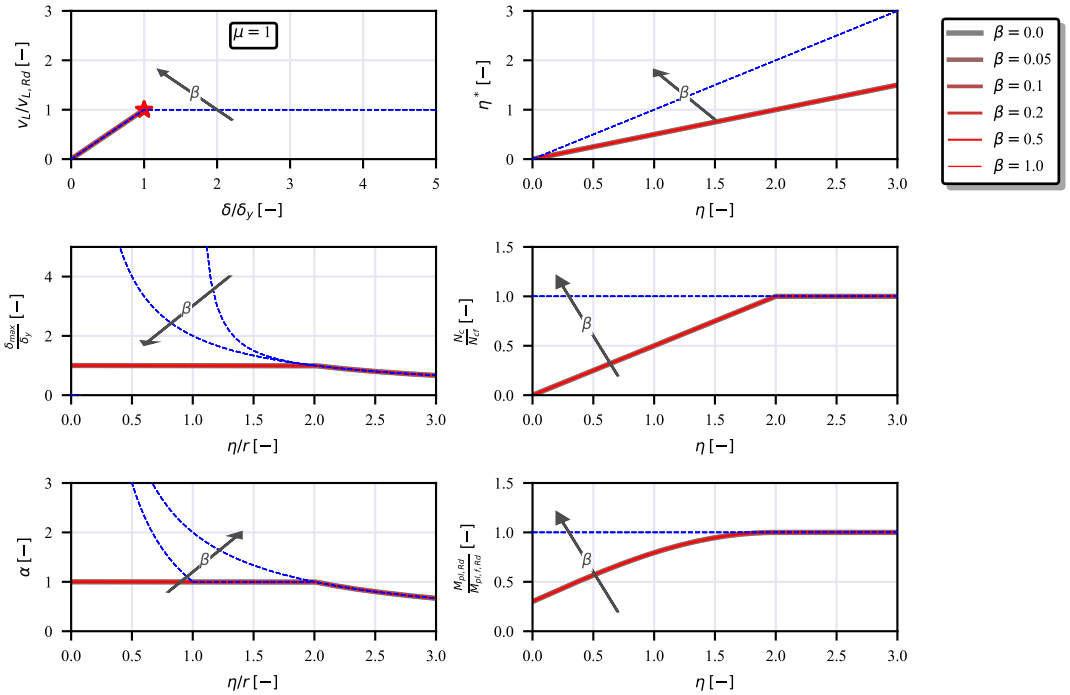

Figure 11 Resulting graphs for variable values of β for the case of fragile (no ductility) shear connection, with $\mu = 1$. Note that as function f of the PSD a specific function is proposed, thus consisting in an example. Therefore the $M_{pl,Rd}$ vs η graph can not be applied generally but specifically relates to the composite section studied and the related PSD function.

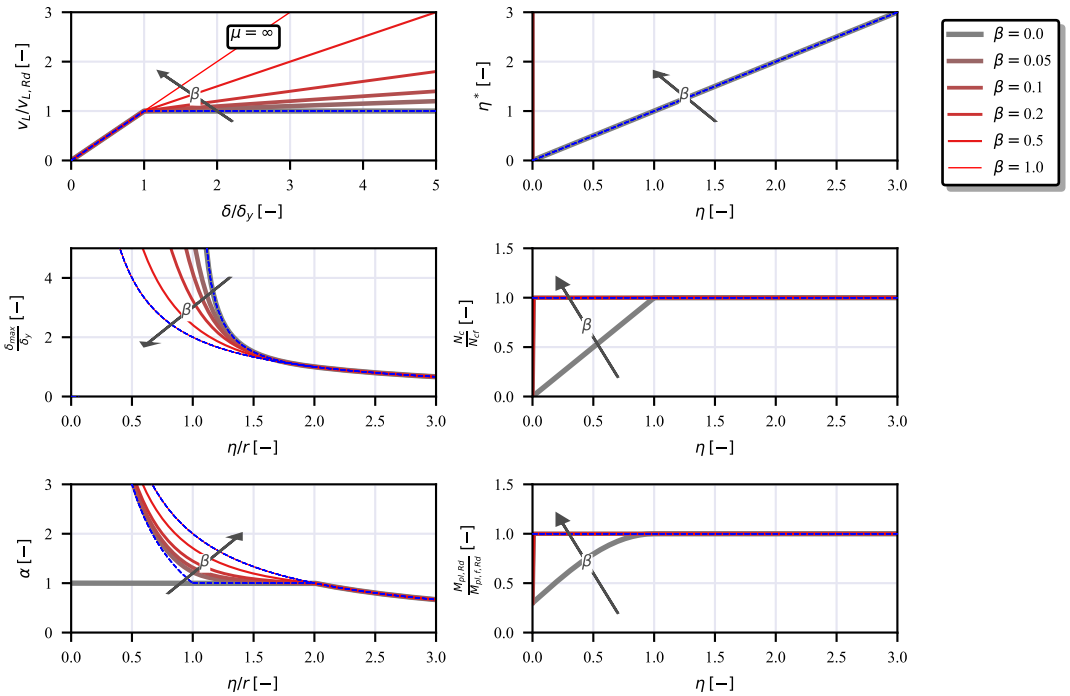

Figure 12 Resulting graphs for variable values of β for the case of infinite redistribution capacity of the shear connection, with $\mu \to \infty$. Note that as function f of the PSD a specific function is proposed, thus consisting in an example. Therefore the $M_{pl,Rd}$ vs η graph can not be applied generally but specifically relates to the composite section studied and the related PSD function.

ANALYTICAL MODEL SUMMARY

- Check hypothesis:
  - uniform shear connection (uniformly spaced, equal shear connectors and constant number of rows);
  - simply supported composite element;
  - uniformly distributed load;
- Input parameters:
  - element geometry: span-length L;
  - shear-connection: yield shear flow $v_{L,y}$, yield slip δ_y, plastic hardening ratio β, ductility μ;
  - composite section: concrete compression force at ULS, FSI N_{cf}, Partial Shear Diagram (PSD) $M_{pl,R} = M_{pl,f,R} \cdot f(N_c/N_{cf})$;
  - composite element: degree of shear connection $\eta = (v_{L,y} \cdot L)/(2N_{cf})$.
  - load ratio: load ratio $r = N_c/N_{cf}$ expressed with reference to the concrete compression force at mid-span under the specified load level N_c.
- Calculation of the non-dimensional parameters Ψ and η^*:

$$\Psi(\mu,\beta) = \frac{\beta(\mu^2 - 2\mu + 1) + 2\mu - 1}{2\mu} \qquad \eta^*(\beta,\eta,\mu) = \eta \cdot \Psi(\mu,\beta)$$

- Calculation of the non-dimensional elastic length

$$\zeta(\beta,\eta/r,\mu) = \max\left(\zeta'(\beta,\eta,r), \zeta''(\mu)\right)$$

$$\zeta'(\beta,\eta,r) = \frac{1 + \beta\eta/r - \eta/r - \sqrt{-\beta\eta^2/r^2 + 2\beta\eta/r + \eta^2/r^2 - 2\eta/r + 1}}{\eta/r(\beta - 1)}$$

$$\zeta'' = 1/\mu$$

- Calculation of the end-slip δ_{max} and overstrength factor α.

$$\left(\frac{\delta_{max}}{\delta_y}\right)(\beta,\eta,r,\mu) = \begin{cases} \frac{1}{\zeta(\beta,\eta,r,\mu)} & 0 \le \eta/r < 2 \\ 2r/\eta & \eta/r \ge 2 \end{cases}$$

$$\alpha(\beta,\eta,r,\mu) = \begin{cases} 1 + \beta\left(\frac{1}{\zeta(\beta,\eta,r,\mu)} - 1\right) & 0 \le \eta/r < 2 \\ 2r/\eta & \eta/r \ge 2 \end{cases}$$

- Maximum transferable force by the shear connection and resistant bending moment on the basis of the Partial Shear Diagram (PSD)

$$N_{c,max}(\beta,\eta,\mu) = \begin{cases} N_{cf} & \eta^* \ge 1 \\ \eta^*(\beta,\eta,\mu)N_{cf} & \eta^* < 1 \end{cases}$$

$$M_R(\beta,\eta,\mu) = f(N_{c,max}(\beta,\eta,\mu)/N_{cf}) \cdot M_{pl,f,R}$$

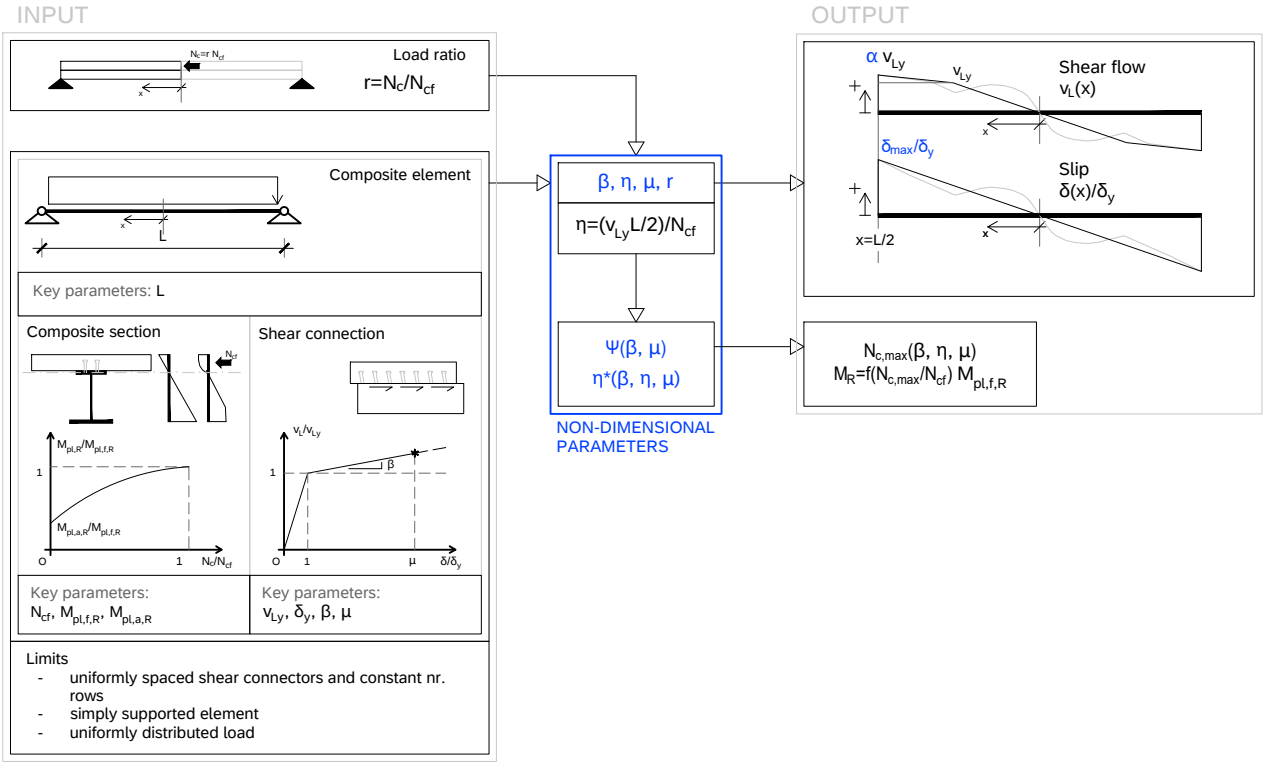

Figure 13 Analytical model summary scheme

4 | COMPARISON WITH NUMERICAL PARAMETRIC ANALYSIS

A numerical 1D method is used to carry out a parametric analysis. The numerical method consists in a finite differences method. The method is explicit and implements the numerical resolution of the problem described in figure 3. It is based on a one-dimensional finite differences method including the shear connection and cross-section non-linearity. It is solving the coupled differential equations (Equations 2, 1) governing the behavior of the composite beam. The numerical method implements a shooting technique. It transforms a Boundary Value Problem (BVP) into an Initial Value Problem (IVP). This consists in changing a first boundary condition in order to respect a second one on the other boundary. The Partial Shear Surface (Equation 8) is numerically derived with a Strain Limited (SL) analysis. This is used as model for the composite section. The shear connection is modelled as Equation 17. No ductility limit μ is put on the slip. Convergence of the iterative method is reached when the the boundary conditions (BCs) are satisfied. The first boundary condition is $\delta(0) = 0$ (absent slip at mid-span). The second boundary condition is $N_c(L/2) = 0$ (absent concrete compression force at support). These BCs are numerically checked within a small tolerance.

The varied parameters are:

$$\begin{aligned} L &= (10)\ m \\ \eta &= (2, 1.8, 1.6, 1.4, 1.2, 1.1, 1, 0.9, 0.8, 0.7, 0.6, 0.5, 0.4, 0.3, 0.2, 0.1) \\ \beta &= (0.001, 0.002, 0.005, 0.01, 0.02, 0.05, 0.1, 0.2, 0.5, 1) \\ \delta_y &= (1, 2)\ mm \\ M(L/2) &= (0.99, 0.9, 0.7, 0.5, 0.3, 0.1) \cdot M_{pl,f,Rd} \end{aligned} \tag{53}$$

By imposing the mid-span bending moment $M(L/2)$ the bending moment diagram is known. The loading ratio r is calculated when convergence of the numerical method is reached. In figures 14 and 15 the comparison between the analytical method and the observed numerical results are shown.

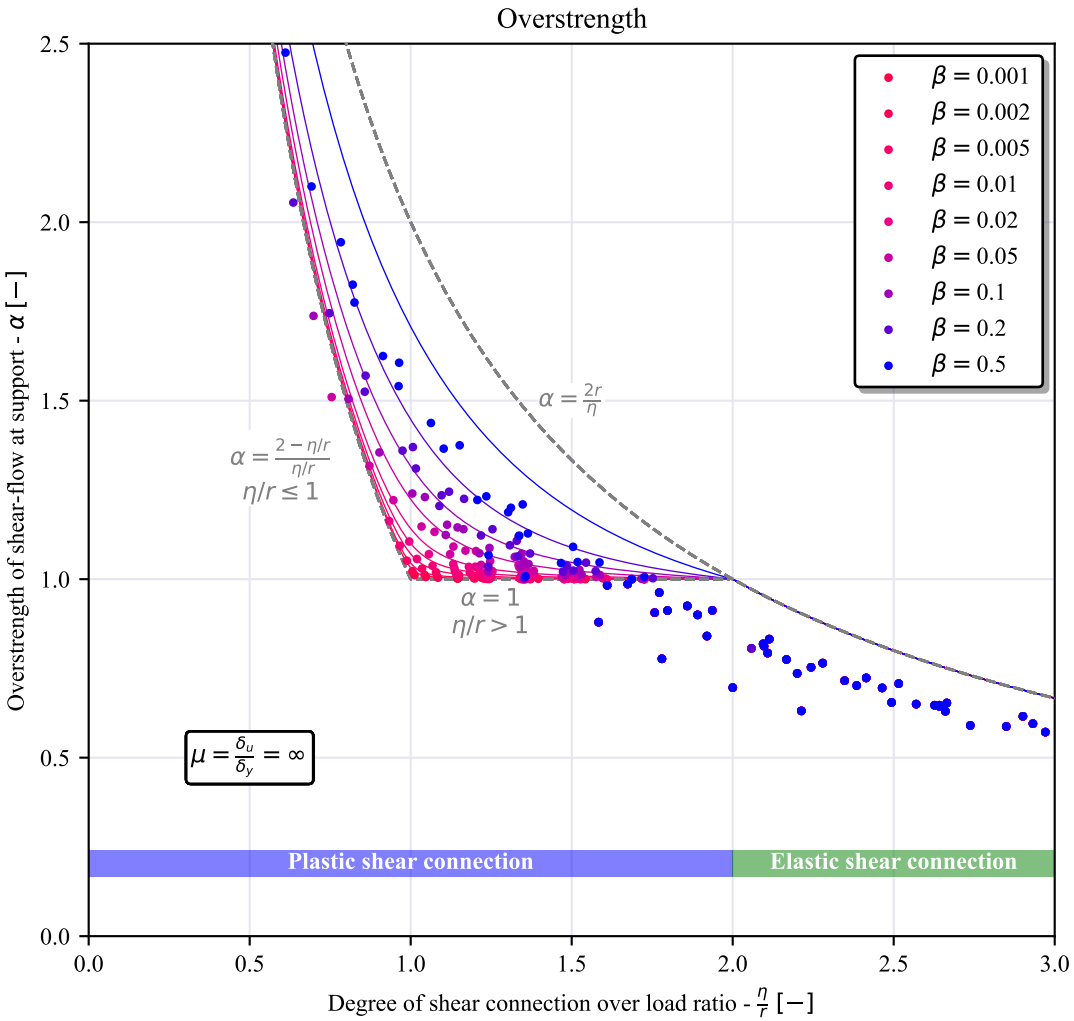

Figure 14 Over-strenght of shear-flow parameter α: comparison of the analytical model predictions (continuous lines) with the numerical results (scatter plot).

5 | DISCUSSION

The proposed analytical model is based on a series of assumptions. These are described in Section . It is mainly limited to simply supported composite beams under uniformly distributed load and evenly spaced shear connectors. A simple bi-linear behavior is used as model for the shear connection. The model synthesizes a series of formulations which aim to predict the mechanical behavior of the composite beam under the given assumptions. The basic governing parameters are the degree of shear connection η, the loading ratio r, the shear connection hardening β and ductility μ. From these a prediction of the end-slip δ_{max}/δ_y can be derived. Moreover using the parameters Ψ and $\eta *$ it is demonstrates how the model converges under notable limit cases to correct predictions in the calculation of the partial shear diagram and of hence the member resistance. The comparison between the analytical method predictions and the numerical analysis, delivers a good outcome. Both the end-slip δ_{max} and the over-strength factor α present an overestimation. The analytical model well describes however the trends of the distributions. And the influence of the non-dimensional parameters clearly emerges in the parametric numerical analysis. Some of the main consequences of the model are:

- the composite beam can be described in non-dimensional terms. This based on the key parameters η (degree of shear connection), r (load ratio as defined by Equation 18). In the analytical model these two parameters play a symmetric role.

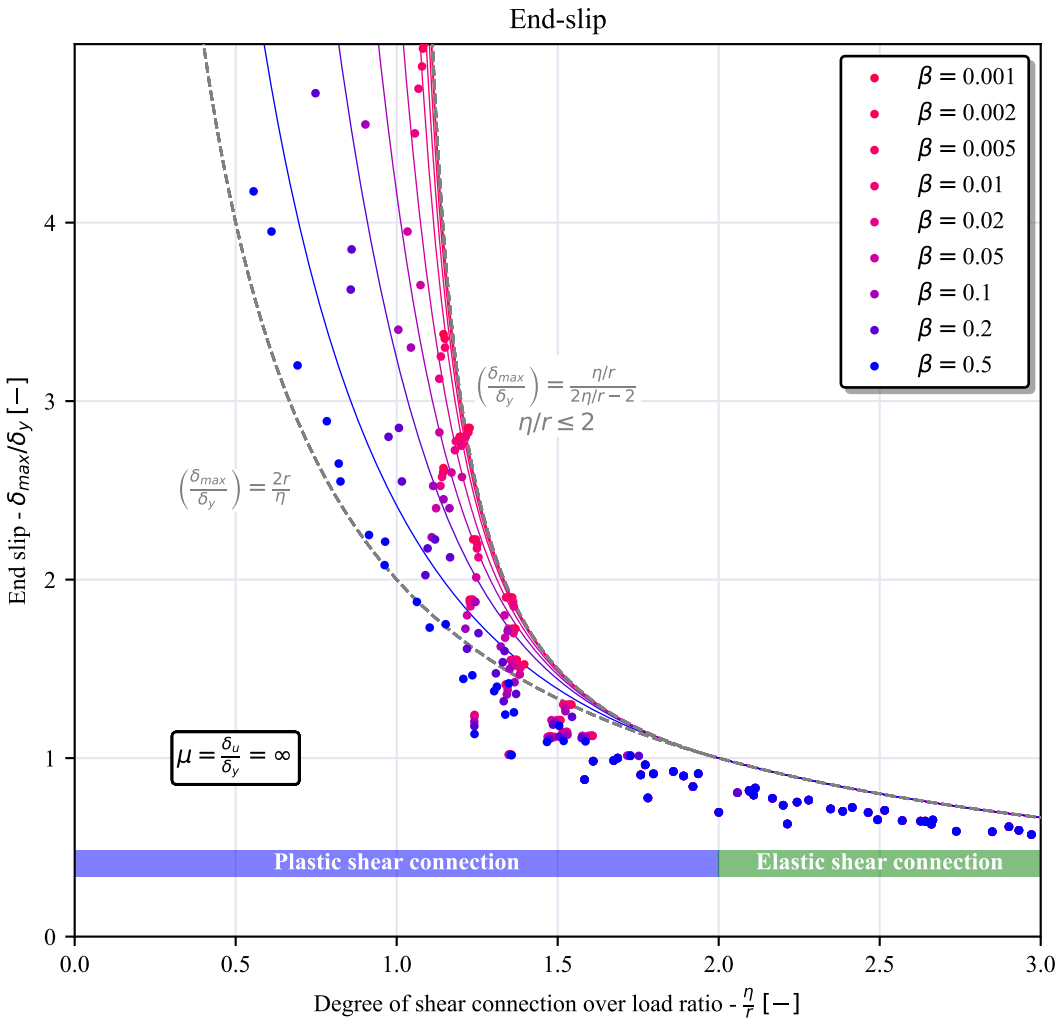

Figure 15 End-slip δ_{max}: comparison of the analytical model predictions (continuous lines) with the numerical results (scatter plot).

The inverse of the load ratio r plays in fact the same role as the degree of shear connection η. The ratio between the end-slip δ_{max} and the yield slip δ_y can be described as function of these non-dimensional terms. The same holds for the over-strength factor $alpha$. It appears that the non-dimensional parameters identified are correctly reducing the the key parameters to the minimum ones. This reflects good in the comparison in the graphs with non-dimensional axes.

- using the plastic hardening parameter β, the analytical model shows how the system shifts from an elastic-perfectly plastic behavior to a perfectly elastic behavior.

- if in the elastic-perfectly plastic (no hardening) case the ductility μ is set as sufficiently high, the model correctly converges to the conventional model of rigid-plastic shear connection. Hence, delivering the same results as the conventional calculations of the composite beam in terms of resistance.

- the Partial Shear Diagram appears in the analytical model as a consequence of the limitation of the slip δ in the limit case of no plastic hardening $\beta = 0$. The analytical model is first elaborated in absence of a slip-limitation in terms of ductility μ. From this, two key-diagrams have been derived. In absence of a slip limitation the model fails to describe the mechanical behavior for the case of $\beta = 0$ (no plastic hardening of the shear connection) and $\eta/r < 1$. This is because the solution to the equilibrium equation 36 does not exist. When a slip limitation μ is introduced for the shear connection, the model well

predicts the existence of the Partial Shear Diagram of composite beams. The necessity for the slip to respect the failure criteria $\delta \leq \mu\delta_y$, imposes a limitation to the beam load capacity. This explains and reproduces the Partial Shear Diagram.

- For $\beta \to 0$ and large but finite values of μ, the model outcomes converge to the conventional rigid-plastic description of the shear connection. This leads the parameter η^* being coincident with the notion of Degree of Shear Connection η. This limit case leads also to the coincidence of the function $M_R(\eta)$ with the notion of Partial Shear Diagram.

- from the comparison between numerical and the analytical predictions that emerges from figure 15, the formula related to the limit $\beta \to 0$, appears to be a reasonable upper limit estimation of the end-slip, thus slip demand on the shear connection. If judged reliable, the formula can be used to calibrate reasonable design rules to impose a sufficient ductility or conversely a minimum degree of shear connection for a specific type of shear connection mean.

- the ductility μ together with the yield slip δ_y (or alternatively the plastic slip capacity δ_u) appear to be key parameters. This evidences a potential lack of the current EC4 [1] which only imposes a minimum value of the plastic slip capacity δ_u to define the shear connectors as ductile. The future version of EC4 at the present version introduces a more complete description of the shear connection in this sense. Probably trying to address this specific problem.

- from comparisons emerging from figure 14 and figure 15, the analytical formulations appear to correctly catch more than the values, the global trends, with the slope and the asymptotic distributions of the trends presenting a substantial agreement.

- two beams of different span-lengths L with same value of Degree of Shear Connection η and same δ_y, v_{Ly}, μ and β, have the same mechanical behavior. These have according to the proposed model, same bending resistance and will exhibit same end-slip. This can be identified as an equivalence principle between composite beams. These two beams would have the same shear connection behavior and would deliver the same slip demand on the shear connection. This would hence not justify a more severe minimum degree of shear connection for the longer beam.

- the analytical simplified model especially demonstrates how one of the key-driving parameter to quantify the end-slip δ_{max} is not the ultimate slip δ_u. In contrary the end-slip can be quantified as a multiple of the value δ_y with this multiple being a function of the non-dimensional parameters η, β, r. The same reasoning holds for the over-strength of the shear flow in the support region. This can be described as a multiple of the value $v_{L,y}$, with the parameter α being this multiple.

- the over-strength factor α is also one of the outcomes of the model. The formulas describe the influence of the different parameters on the longitudinal shear in the support region. This can in the future help understanding the effect of plastic hardening of connectors for the longitudinal shear verification in the support region.

The method is not suitable for predicting the load-slip behavior for load distributions different from uniformly distributed. The extension of it to other load distributions can however be evaluated in future works. It is supposed here that the method can be generalized to a generic behavior of the shear connection $P(\delta)$. In synthesizing the numerical method, a bi-linear mechanical model was used. A second order equation was emerging from the equilibrium equation and this was allowing to analytically find the roots as ζ. The process can be extended to a generic reasonable function $P(\delta)$. This function can for example be derived from real push out-test. In such case, a numerical method is more suitable to find the roots of ζ. Similar extension can be done with the parameter Ψ as defined by the integral in equation 26 and subsequent derivation of η^*. The assumption that the method is extendable to a generic $P(\delta)$ needs however still to be verified. Numerical and possible tests have to be done in the future to ascertain the reliability of the method. The assertion is aimed mostly as input for further research works.

6 | CONCLUSIONS

An analytical model representing the behavior of a simply supported composite beam under uniformly distributed load has been synthesized. A uniform shear connection is considered on the longitudinal axis. A bi-linear elastic with plastic hardening behavior is used and the ductility is also included. The model formulation is summarized in Section 3.4. It is built on the simplification assumption of constant strain slip ($\epsilon_{slip} = const.$). Despite the limitations and the simplification assumptions, the model is coherent and consistent. Interestingly it shows how it connects in specific limit cases to the rigid-perfectly plastic or perfectly elastic hypothesis. The model predictions are compared with numerically derived results. Qualitatively the global trends

are well predicted by the analytical model. If judged reliable, the model can further improve the understanding the behavior of composite steel-concrete beams. Further research is needed to judge weather the model is delivering reliable results. It tries to describe the composite member in non-dimensional terms, reducing the number of degrees of freedom describing the problem to the minimum. It can be potentially used to predict the beam end-slip, thus helping calibrating design rules for a minimum degree of shear connection to prescribe in the codes. Equivalently it can help to judge specific connection means present sufficient ductility based on their first yield point. The influence of the hardening factor on the overs-strength of longitudinal shear at the support is also modeled. The related formula can help calibrating reliable design rules to perform the longitudinal shear check in the support region. This is currently object of study for the implementations of future generation of EC4.

6.1 | Acknowledgements

The present article is not sustained by any research fund.

6.2 | Bibliography

References

1. Standard B. Eurocode 4: Design of composite steel and concrete structures. Part. 2004;**1**(1).

2. Johnson RP. Composite Structures of Steel and Concrete: beams, slabs, columns and frames for buildings. John Wiley & Sons; 2018.

3. Johnson RP, Molenstra N, and EPPIB. Partial shear connection in composite beams for buildings. Proceedings of the Institution of Civil Engineers. 1991;**91**(4):679–704.

4. Classen M. Limitations on the use of partial shear connection in composite beams with steel T-sections and uniformly spaced rib shear connectors. Journal of Constructional Steel Research. 2018;**142**:99–112.

5. Bärtschi R. Load bearing behaviour of composite beams in low degrees of partial shear connection. 290. vdf Hochschulverlag AG; 2005.

6. Zhang Q. Moment and Longitudinal Resistance for Composite Beams Based on Strain Limited Design Method. University of Luxembourg, Luxembourg, Luxembourg; 2020.

Nomenclature

$(1/r)_u$	ultimate curvature
$1/r$	curvature
α	shear-flow over-strength at support
β	hardening factor
δ	slip
δ_y	yield slip
ϵ_{slip}	slip strain
η	degree of shear connection
η^*	non-dimensional capacity of shear connection
μ	ductility

330	ϕ	rotation
331	Ψ	non-dimensional integral of the shear flow-slip model
332	e_x	shear connectors spacing
333	f	Partial Shear Diagram normalized function
334	L	span length
335	M	bending moment
336	$M_{pl,f,R}$	resistant plastic bending moment in full shear connection
337	M_R	resistant bending moment of the composite element
338	n	number of shear connectors
339	N_c	resultant of compression force on the concrete part of the section
340	n_f	number of shear connectors for Full Shear Connection
341	$N_{c,max}$	maximum concrete compression force transferable by the shear connection
342	N_{cf}	resultant of compression force on the concrete part of the section at ULS in Full Shear Interaction conditions
343	P	bearing force in the single shear connector row
344	P_y	yield bearing force in the single shear connector row
345	q	uniform load
346	r	loading ratio
347	v_L	longitudinal shear-flow
348	$v_{L,y}$	yield longitudinal shear flow
349	w	deflection
350	x	Coordinate of section from mid-span
351	x_y	yield point coordinate of section from mid-span

How to cite this article: Profico F., and Zanon R. (2023), An Analytical Model of Simply Supported Steel-Concrete Composite Beam With Bi-Linear Behavior of the Shear Connection Including Ductility: Formulation and Comparison With Numerical Results, *The journal*, *2017;00:1–6*.